

Chapter 8

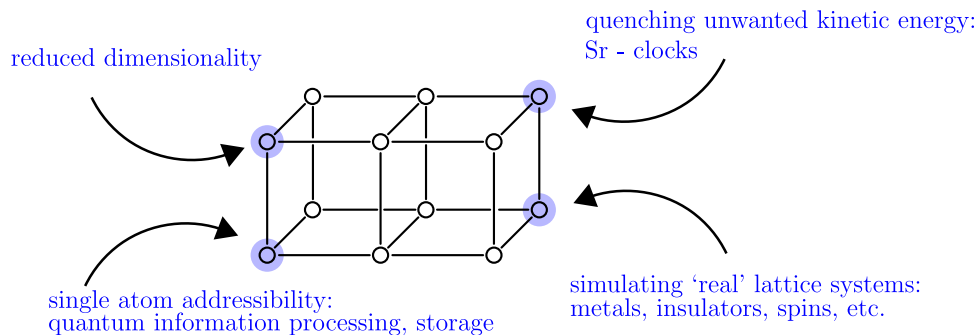
Optical lattices

Learning goals

- What is an optical lattice?
- What phases does the Bose Hubbard model have?
- How do you characterize the excitations in the Mott insulator?
- How do you derive the long-wavelength theory of the weakly interacting superfluid?
- How do you derive the long-wavelength theory of the transition point?
- What is a Higgs mode?

8.1 Motivation

There are many reasons why one would want to study atoms in artificial lattice potentials. The following figure highlights a few of them.



8.2 The lattice potential

In order to discuss lattice systems we need a potential for the trapped atoms that resembles the periodic potential felt by the electrons in solids. In most current applications the optical dipole force of a spatially varying electric field is used

$$\mathbf{F} = \frac{1}{2} \alpha(\omega_L) \nabla I(\mathbf{r}). \quad (8.1)$$

Only the time-averaged intensity

$$I(\mathbf{r}) = \frac{\omega_L}{2\pi} \int_0^{2\pi/\omega_L} dt |\mathbf{E}(\mathbf{r}, \mathbf{t})|^2 \quad (8.2)$$

enters this expression as the motion of the atoms in the light field are much smaller than the typical laser-frequency ω_L . The pre-factor $\alpha(\omega_L)$ is given by the polarizability of the atoms which depends on the detuning $\Delta = \omega_{\text{atom}} - \omega_L$

$$\alpha(\omega_L) \approx \frac{|\langle e | \hat{\mathbf{d}}_{\mathbf{E}} | g \rangle|^2}{\Delta} \quad \Rightarrow \quad V(\mathbf{r}) \approx \frac{I(\mathbf{r})}{\Delta}, \quad (8.3)$$

where $\hat{\mathbf{d}}_{\mathbf{E}}$ is the dipole operator in the direction of the field and $|g\rangle$ and $|e\rangle$ are the two atomic states separated by ω_{atom} . From this expression we see that the optical dipole force gives rise to a potential which can either be attractive or repulsive depending on the detuning Δ . We speak of a

red lattice:	$\Delta < 0$	atoms sit at maxima of the field,
blue lattice:	$\Delta > 0$	atoms sit at the minima of the field.

If we now want to obtain a *periodic potential* we need a periodic electric field. One way to achieve this is to overlap two counter-propagating lasers to create a standing wave and hence

$$V(r, z) = V_0 e^{-2r^2/w^2(z)} \sin^2(kz), \quad k = \frac{2\pi}{\lambda}. \quad (8.4)$$

Here, z is the direction of the laser and $r = \sqrt{x^2 + y^2}$ the radius perpendicular to it; λ is the wavelength and $w(z)$ the waist profile of the laser. If one superimposes crossed laser beams in several directions we arrive at a potential of the form

$$V(\mathbf{r}) = \sum_{i=1}^d V_0^i \sin(k_i r_i). \quad (8.5)$$

Generically, the strength of the optical potential are given in recoil energies

$$\frac{V_0^i}{E_r^i} = \frac{V_0^i}{\frac{\hbar^2 k_i^2}{2m}} \approx 0 \dots 20, \quad (8.6)$$

where 20 recoils energies corresponds to a fairly strong lattice.

8.3 Band structure

When we want to discuss lattice problems we try to cast to full problem of the free kinetic energy $-\hbar^2 \nabla^2 / 2m$ together with the potential energy $V(\mathbf{r})$ into a simple tight-binding model of the form

$$H = -t \sum_{\langle i, j \rangle} a_i^\dagger a_j. \quad (8.7)$$

We hope to capture the dynamics on the lattice by hops between nearest neighbor lattice sites $\langle i, j \rangle$ only. In the following we show how we can derive such a single-band tight-binding model. We are facing the following problem

$$\left[-\frac{\hbar^2}{2m} (\partial_x^2 + \partial_y^2 + \partial_z^2) + V(\mathbf{r}) \right] \Psi(x, y, z) = E \Psi(x, y, z). \quad (8.8)$$

In a first step we separate the different spatial directions

$$\Psi(x, y, z) = \psi_x(x) \psi_y(y) \psi_z(z). \quad (8.9)$$

This allows us to concentrate on one-dimensional problems alone

$$\left[-\frac{\hbar^2}{2m} \partial_x^2 + V_0 \cos(qx) \right] \psi_x(x) = E \psi_x(x). \quad (8.10)$$

To solve this problem we can go along three different routes

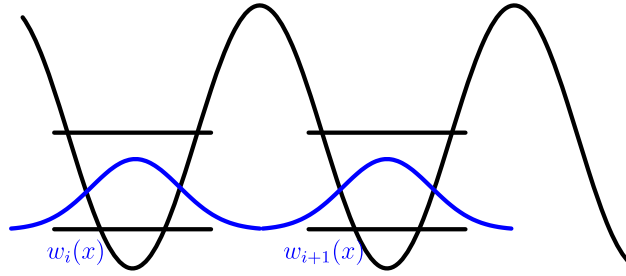


Figure 8.1: **Tight binding**. Schematic view of the lowest harmonic oscillator wave function in each potential well.

1. Use the exact solution to (8.10), which is also known as the Mathieu equation.
2. Numerically solve (8.10).
3. Map to a simple tight-binding model.

We first employ a simple toy version of a tight-binding model and then link the effective parameters in this toy model to the real problem by matching it to the solution (numerical or exact) of the full problem.

In a tight-binding model we assume that we can think of each potential minimum as an approximate harmonic oscillator, cf. Fig. 8.1. However, there will be a finite tunneling rate due to wave-function overlaps. This immediately leads to a Hamiltonian for two sites that looks qualitatively like

$$H = -t|i\rangle\langle i+1| - t|i+1\rangle\langle i| = \begin{pmatrix} 0 & -t \\ -t & 0 \end{pmatrix}, \quad (8.11)$$

where i labels the sites and t is the “tunneling” coefficient. We have to determine t from a more accurate description than the harmonic oscillator wells adjacent to each other. To do so we make use of some general properties of problems with a discrete translation symmetry.

If we have a periodic potential $V(x) = V(x+a)$, where a is the lattice constant $a = 2\pi/q = \pi/k$, we know that the solutions of the Schrödinger equation fulfill (Bloch theorem)

$$\phi_{n,p}(x) = e^{ipx} u_{n,p}(x) \quad \text{with} \quad u_{np}(x) = u_{np}(x+a), \quad \text{and} \quad p \in \left[-\frac{\pi}{a}, \frac{\pi}{a}\right], \quad n = 1, 2, 3, \dots \quad (8.12)$$

Here, p is called the lattice momentum which tells us how the phase changes from “site” to “site” and $u_{np}(x)$ has the periodicity of the lattice. The functions $u_{np}(x)$ can now be obtained either from exact solutions or numerical simulations. In either case we make use of the important concept of *Wannier functions*

$$w_{n,i}(x) = w_n(x - x_i) = \int_{-\pi/a}^{\pi/a} \frac{dp}{2\pi} \phi_{n,p}(x) e^{-ix_i p}. \quad (8.13)$$

These functions have the following properties:

1. They are centered around the potential minima at $x_i = na$ with $n \in \mathbb{Z}$.
2. They fall off exponentially.
3. They form an orthonormal set.

Owing to the last property we can make use of them to rewrite the field operators

$$\hat{\psi}(x) = \sum_{n,i} w_{n,i}^*(x) \hat{a}_{n,i}, \quad (8.14)$$

where $\hat{a}_{n,i}^\dagger$ creates a particle in the n 'th band at site i . We now rewrite the second quantized Hamiltonian in the new basis

$$H = \int dx \hat{\psi}^\dagger(x) \left[-\frac{\hbar^2}{2m} \partial_x^2 + V(x) \right] \hat{\psi}(x) \quad (8.15)$$

$$= \sum_{ijnm} \hat{a}_{n,i}^\dagger \hat{a}_{m,j} \int dx w_n(x-x_i) \left[-\frac{\hbar^2}{2m} \partial_x^2 + V(x) \right] w_m^*(x-x_j) \quad (8.16)$$

$$= \sum_{ijn} \hat{a}_{n,i}^\dagger \hat{a}_{n,j} \int dx w_n(x-x_i) \left[-\frac{\hbar^2}{2m} \partial_x^2 + V(x) \right] w_n^*(x-x_j) \quad (8.17)$$

$$\approx \sum_{in} \left(\hat{a}_{n,i}^\dagger \hat{a}_{n,i+1} + a_{n,i+1}^\dagger a_{n,i} \right) \underbrace{\int dx w_n(x-x_i) \left[-\frac{\hbar^2}{2m} \partial_x^2 + V(x) \right] w_n^*(x-x_{i+1})}_{-t} \quad (8.18)$$

$$\approx -t \sum_{\langle i,j \rangle} \hat{a}_i^\dagger \hat{a}_j. \quad (8.19)$$

From the second to the third line we used the fact the the Wannier functions are built from different bands n and the operator in the square brackets does not mix different bands. From line three to four we used the fact that the Wannier functions are exponentially localized. In the last line we also confine ourselves to the lowest band and drop the band index n . These approximations allow us to identify t with a property of the exact solution.

To finish this section we diagonalize the tight-binding Hamiltonian using again Bloch waves

$$\hat{a}_i = \frac{1}{\sqrt{N}} \sum_k \hat{a}_k e^{ikx_i}, \quad (8.20)$$

where N are the number of lattice sites. Inserted into (8.19) we obtain

$$H = -t \sum_{\langle i,j \rangle} \hat{a}_i^\dagger \hat{a}_j = -\frac{t}{N} \sum_{k,k'} \hat{a}_k^\dagger \hat{a}_{k'} \sum_{\langle i,j \rangle} e^{ikr_i - ik'r_j} = \sum_k -2t \cos(ka) \hat{a}_k^\dagger \hat{a}_k = \sum_k \epsilon(k) \hat{a}_k^\dagger \hat{a}_k. \quad (8.21)$$

Hence, we see that the tight-binding approximation amounts to reduce the dispersion relation to the first harmonic, i.e., a simple cosine. Taking further range hopping into account would contribute higher harmonics to the dispersion relation $\epsilon(k)$. With this we conclude our discussion of how to derive a simple lattice model for atoms in an optical lattice. In a next step we take interactions into account.

8.4 The Bose Hubbard model

We model the interactions between the atoms with the simple contact pseud-potential derived in Chp. 2

$$V(\mathbf{r}) = \frac{4\pi\hbar^2 a_s}{2m} \delta(\mathbf{r}). \quad (8.22)$$

Expressed in second quantized form we can again make use of the basis transformation to the Wannier basis

$$H_{\text{int}} = \frac{4\pi\hbar^2 a_s}{2m} \int d\mathbf{r} \hat{\psi}^\dagger(\mathbf{r}) \hat{\psi}^\dagger(\mathbf{r}) \hat{\psi}(\mathbf{r}) \hat{\psi}(\mathbf{r}) \quad (8.23)$$

$$= \frac{4\pi\hbar^2 a_s}{2m} \sum_{i,j,l,m} \hat{a}_i^\dagger \hat{a}_j^\dagger \hat{a}_l \hat{a}_m \int d\mathbf{r} w_i(\mathbf{r}) w_j(\mathbf{r}) w_n^*(\mathbf{r}) w_m^*(\mathbf{r}) \quad (8.24)$$

$$\approx \sum_i \hat{a}_i^\dagger \hat{a}_i^\dagger \hat{a}_i \hat{a}_i \underbrace{\frac{4\pi\hbar^2 a_s}{2m} \int d\mathbf{r} |w_i(\mathbf{r})|^4}_{U/2} = \frac{U}{2} \sum_i \hat{a}_i^\dagger \hat{a}_i (\hat{a}_i^\dagger \hat{a}_i - 1). \quad (8.25)$$

Together with the hopping part derived above we arrive at the single band Bose Hubbard model

$$H_{\text{BH}} = -t \sum_{\langle i,j \rangle} \hat{a}_i^\dagger \hat{a}_j + \frac{U}{2} \sum_i \hat{a}_i^\dagger \hat{a}_i (\hat{a}_i^\dagger \hat{a}_i - 1) - \mu \sum_i \hat{a}_i^\dagger \hat{a}_i, \quad (8.26)$$

where we added a chemical potential term $\propto \mu$. To complete our derivation of the Bose Hubbard model we state the values for t and U as extracted from the exact solution of the Matthieu equation

$$t = \frac{4}{\sqrt{\pi}} E_r \left(\frac{V_0}{E_r} \right)^{3/4} \exp \left[-2 \left(\frac{V_0}{E_r} \right)^{1/2} \right], \quad (8.27)$$

$$U = \sqrt{32\pi} \frac{a_s}{\lambda} E_r \left(\frac{V_0}{E_r} \right)^{3/4}. \quad (8.28)$$

8.4.1 Phase diagram

Superfluid

To gain an understanding of the phase diagram of the Bose Hubbard model (8.26) we start by looking at limiting cases. The simplest case is that of vanishingly small interactions $t \gg U$. In that case it is a good starting point to write for the ground state

$$|\Psi_{\text{SF}}\rangle = \frac{(\hat{a}_{\mathbf{k}=0}^\dagger)^{N\rho}}{\sqrt{(N\rho)!}} |0\rangle, \quad (8.29)$$

where ρ is the density of particles.¹ This wave function describes a simple Bose Einstein Condensate and indicates a superfluid phase. To further characterize this states, let us calculate the probability to find n_i particles on site i . To this end we write the wave function in position space

$$|\Psi_{\text{SF}}\rangle = \frac{1}{\sqrt{(N\rho)!}} \left[\sum_i \hat{a}_i^\dagger \right]^{N\rho} |0\rangle = \frac{1}{\sqrt{(N\rho)! N^{N\rho}}} \sum_{\tilde{\alpha}} \frac{(N\rho)!}{\alpha_1! \dots \alpha_N!} \prod_{i=1}^N (b_i^\dagger)^{\alpha_i} |0\rangle. \quad (8.30)$$

Here $\tilde{\alpha}$ is a multi-index with the sum over all indices equal to $N\rho$, i.e. $\tilde{\alpha} \in \mathcal{A} = \{\tilde{\alpha} = (\alpha_1, \alpha_2, \dots, \alpha_N) \in \mathbb{N}^N | \sum_i \alpha_i = N\rho\}$. The density matrix of the ground state is now in the desired form to carry out the partial trace over all but one site. The density matrix writes to

$$\rho_{SF} = |\Psi_{\text{SF}}\rangle \langle \Psi_{\text{SF}}| = \frac{(N\rho)!}{N^{N\rho}} \sum_{\alpha, \beta} \frac{1}{\sqrt{\alpha_1! \dots \beta_N!}} |\alpha\rangle \langle \beta|, \quad (8.31)$$

where α, β are again in \mathcal{A} and $|\alpha\rangle$ denotes the normalized state

$$|\alpha\rangle = \prod_{i=1}^N \frac{(b_i^\dagger)^{\alpha_i}}{\sqrt{\alpha_i!}} |0\rangle. \quad (8.32)$$

If the occupation of the site i in $|\alpha\rangle$ is fixed to n_i , the remaining sites of $|\alpha\rangle$ are carrying $N\rho - n_i$ particles. States in with another number of particles are orthogonal to the states with $N\rho - n_i$ particles. Therefore only states $|\beta\rangle$ with $N\rho - n_i$ particles contribute to the partial trace, leading to a diagonal density matrix. The diagonal elements of ρ_i are equal to

$$\frac{(N\rho)!}{N^{N\rho}} \frac{1}{n_i!} \sum_{\tilde{\alpha}'} \frac{1}{\alpha_1! \dots \alpha_{i-1}! \alpha_{i+1}! \dots \alpha_N!} = \frac{1}{n_i!} \frac{(N\rho)!}{(N\rho - n_i)!} \frac{(N-1)^{N\rho - n_i}}{N^{N\rho}}. \quad (8.33)$$

¹We assume ρN to be an integer number.

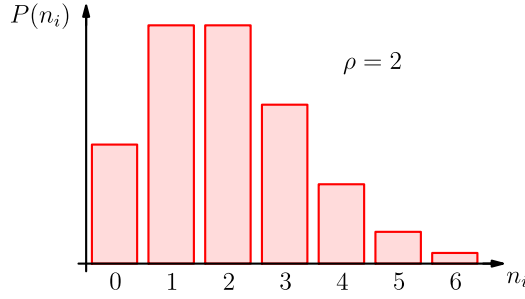


Figure 8.2: **Number fluctuations.** Probability to find n_i particles on any given site assuming a mean density ρ . We see that the Poissonian distribution in the superfluid leads to large particle number fluctuations.

The $\tilde{\alpha}'$ are in the set $\mathcal{A}' = \{\tilde{\alpha} = (\alpha_1, \dots, \alpha_{i-1}, \alpha_{i+1}, \dots, \alpha_N) \in \mathbb{N}^{N-1} | \sum_i' \alpha_i = N\rho - n_i\}$. In the limit of large N Stirling's formula can be used and the distribution function $P(n_i)$ becomes Poissonian

$$P(n_i) = \frac{e^{-\rho} \rho^{n_i}}{n_i!}. \quad (8.34)$$

As we can see in Fig. 8.2, this distribution is fairly wide, i.e., for a mean particle number $\rho = 2$ there is an appreciable probability to find zero, one, etc. particles per site. We will see in the following that for strong interactions $U \gg t$ such particle number fluctuations are unfavorable.

Mott insulator

If we turn to the other extreme where $U \gg t$ we can start from $t \equiv 0$. In this case any number state is an eigenstate of the Hamiltonian and there are no terms coupling different sites. Hence, our problem factorizes into single site problems and $\rho \in \mathbb{N}$. In order to determine the optimal filling ρ per site we compare the energies

$$E_i = \frac{U}{2} \rho(\rho - 1) - \mu\rho \quad \Rightarrow \quad (\rho - 1)U < \mu < \rho U. \quad (8.35)$$

We see that as a function of the chemical potential the density ρ is jumping in discrete steps. Moreover, for most values of μ we observe that the compressibility

$$\kappa \propto \frac{\partial \rho}{\partial \mu} = 0, \quad (8.36)$$

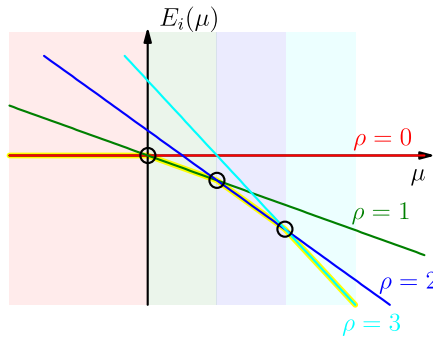


Figure 8.3: **Local energies.** The energy of different number states as a function of chemical potential. The circles indicate “transitions” where a change in the number of atoms in the minimal energy state happens.

i.e., we deal with a series of incompressible states called *Mott insulator states*.

In order to take a finite hopping amplitude t into account we start from the localized states and build a variational wave function on that. We still assume the state to be site factorized, however, with a potential mixture of different numbers states per site

$$|\Psi\rangle = \prod_i |\psi_i\rangle \quad \text{where} \quad |\psi_i\rangle = \cos(\vartheta/2) |\rho\rangle_i + \frac{\sin(\vartheta/2)}{\sqrt{2}} [|\rho+1\rangle_i + |\rho-1\rangle_i]. \quad (8.37)$$

With this ansatz we confine ourselves to integer filling ρ as $|\rho \pm 1\rangle$ are admixed equally. In order to find the optimal values of the variational parameters ϑ we have to minimize the energy

$$\partial_{\vartheta} \langle \Psi | H_{\text{BH}} | \Psi \rangle = 0. \quad (8.38)$$

We start with the local terms

$$\begin{aligned} E_{\text{loc}} &= \langle \psi_i | \frac{U}{2} \hat{a}_i^\dagger \hat{a}_i (\hat{a}_i^\dagger \hat{a}_i - 1) - \mu \hat{a}_i^\dagger \hat{a}_i | \psi_i \rangle = \frac{U}{2} [\rho(\rho-1) + \sin^2(\vartheta/2)] - \mu\rho \\ &\approx \frac{U}{2} \rho(\rho-1) - \mu\rho + \frac{U}{8} \vartheta^2. \end{aligned} \quad (8.39)$$

In the last line we expanded in small ϑ as we are interested in the physics close to the localized phase. For the evaluation of the kinetic energy we first calculate the superfluid order parameter

$$\langle \Psi | \hat{a}_i | \Psi \rangle = \frac{\sin(\vartheta/2) \cos(\vartheta/2)}{\sqrt{2}} (\sqrt{\rho} + \sqrt{\rho+1}) \approx \frac{\vartheta}{2\sqrt{2}} (\sqrt{\rho} + \sqrt{\rho+1}) \equiv \psi. \quad (8.40)$$

As the full wave function is a product state, $|\Psi\rangle = \prod_i |\psi_i\rangle$, the kinetic energy expectation value reduces to

$$\langle \Psi | \hat{a}_i^\dagger \hat{a}_j | \Psi \rangle = \psi^2 \quad \Rightarrow \quad E_{\text{kin}} \approx -tz \frac{\vartheta^2}{8} (\sqrt{\rho} + \sqrt{\rho+1})^2, \quad (8.41)$$

where z is the number of nearest neighbors on the lattice. We now obtain for the variational energy

$$E_{\text{var}}(\vartheta) = \frac{U}{2} \rho(\rho-1) - \mu\rho + \frac{\vartheta^2}{2} \left[\frac{U}{4} - tz (\sqrt{\rho} + \sqrt{\rho+1})^2 \right]. \quad (8.42)$$

In a Ginzburg-Landau logic we are now tracking a sign-change of the quadratic coefficient to find the phase boundary between the Mott insulator and the superfluid

$$\left. \frac{U}{tz} \right|_{\text{crit}} = (\sqrt{\rho} + \sqrt{\rho+1})^2. \quad (8.43)$$

This result gives us the transition between a Mott insulator and a superfluid only at integer filling. In order to find the full phase diagram we have to generalize our trial wave function to include different fillings

$$|\psi_i\rangle = \cos(\vartheta/2) |\rho\rangle_i + \sin(\vartheta/2) [\cos(\chi/2) |\rho+1\rangle_i + \sin(\chi/2) |\rho-1\rangle_i]. \quad (8.44)$$

We leave the details of the calculation as an exercise and only present the solution for the phase boundaries, cf. Fig. 8.4

$$\mu_{\text{crit}}^\pm = \rho U - \frac{U}{2} - \frac{1}{2} \left[tz \pm \sqrt{1 - tz(1+2\rho) + (tz)^2} \right], \quad (8.45)$$

where $\rho \in \mathbb{N}$ is the integer number characterizing the ρ 'th *Mott lobe*.

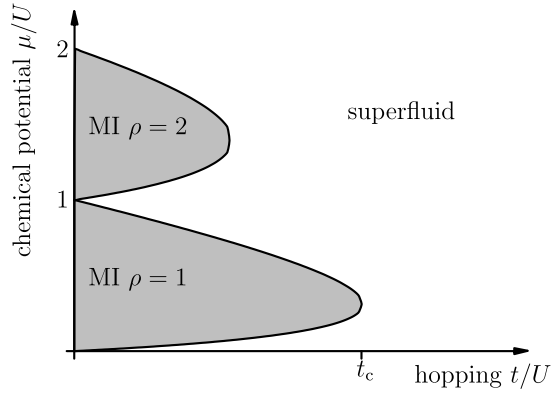


Figure 8.4: **Mott lobes.** Phase diagram of the Bose Hubbard model as a function of hopping and chemical potential. In gray the Mott insulating phases surrounded by the superfluid region.

8.4.2 Excitations

After understanding the ground state phase diagram of the Bose Hubbard model (8.26) we try to address the excitation spectrum. The weakly interacting superfluid we already covered in Chap. 6: The low lying excitations are phonons, the Goldstone modes of the broken U(1) symmetry. Let us construct a simple toy model to understand the excitations in the Mott insulating phase.

The Mott insulator in the $t \rightarrow 0$ limit has exactly one (an integer number of) particle(s) per site. We start from this limit to construct the Hilbert-space for the low-lying excitations. We construct a *particle* state

$$|P_i\rangle = \hat{p}_i^\dagger |\text{Mott}\rangle = \left[\begin{array}{|c|c|c|c|c|c|} \hline \circ & \circ & \overset{\circ}{\circ} & \circ & \circ & \circ \\ \hline \end{array} \right] \Rightarrow \hat{a}_j^\dagger \hat{a}_i |P_i\rangle = \rho |P_j\rangle, \quad (8.46)$$

and likewise a hole state

$$|H_i\rangle = \hat{h}_i^\dagger |\text{Mott}\rangle = \left[\begin{array}{|c|c|c|c|c|c|} \hline \circ & \circ & \square & \circ & \circ & \circ \\ \hline \end{array} \right] \Rightarrow \hat{a}_j^\dagger \hat{a}_i |H_i\rangle = (\rho - 1) |H_j\rangle, \quad (8.47)$$

The above equations define the operators \hat{h}_i and \hat{p}_i . We can now write down the kinetic energy part of our effective low-energy particles

$$H_{\text{MI}}^{\text{kin}} = -t\rho \sum_{\langle i,j \rangle} \hat{p}_i^\dagger \hat{p}_j - t(\rho - 1) \sum_{\langle i,j \rangle} \hat{h}_i^\dagger \hat{h}_j, \quad (8.48)$$

where we see that particles and holes have a different hopping amplitude due to the different bosonic enhancement factor ρ versus $\rho - 1$. We can also write down the local energies

$$H_{\text{MI}}^{\text{kin}} = \sum_i \left(\frac{U}{2} - \delta\mu \right) \hat{p}_i^\dagger \hat{p}_i + \sum_i \left(\frac{U}{2} + \delta\mu \right) \hat{h}_i^\dagger \hat{h}_i, \quad (8.49)$$

where we introduced $\delta\mu = \mu - U(\rho - 1)$. We can now diagonalize $H_{\text{MI}} = H_{\text{MI}}^{\text{kin}} + H_{\text{MI}}^{\text{lc}}$ to find

$$\epsilon_{\text{p}}(\mathbf{k}) = \frac{U}{2} - \delta\mu - 2t\rho \sum_{i=1}^d \cos(k_i a), \quad (8.50)$$

$$\epsilon_{\text{h}}(\mathbf{k}) = \frac{U}{2} + \delta\mu - 2t(\rho - 1) \sum_{i=1}^d \cos(k_i a). \quad (8.51)$$

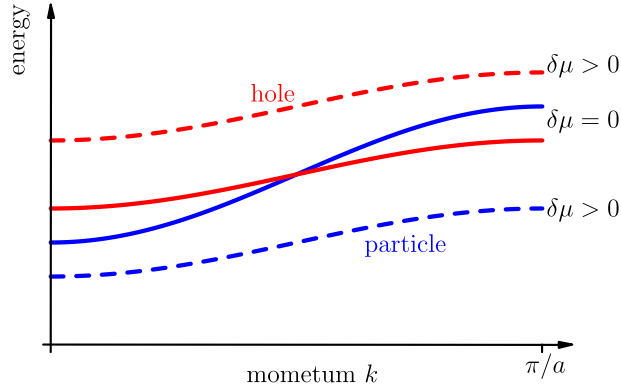


Figure 8.5: **Excitations in the Mott insulator.** For $\delta\mu = 0$ and $t < t_c$, both particle (solid blue) and hole (solid red) excitations are gapped. For $\delta\mu > 0$ (dashed lines), the gap of the particle excitation is getting smaller and eventually closes at the phase boundary. Similarly for $\delta\mu < 0$, the hole gap is getting smaller.

The two dispersions are shown in Fig. 8.5. Both particles and holes are gapped in the Mott phase. However, we see that for $\delta\mu \gg 0$, the particle excitations close their gap, i.e., particles condense. This happens along to upper phase boundary in Fig. 8.4. For $\delta\mu \ll 0$, on the other hand, holes condense. Moreover, there is a critical $\delta\mu = \delta\bar{\mu}$, where both particles and holes close their gap together. This is the tip of the Mott lobe where the density does not change across the phase boundary.

These excitation spectra were calculated assuming a *non-fluctuating*, classical, ground-state. In a more realistic approach one would take such fluctuations into account via a specialized Bogoliubov method which is beyond the scope of this lecture. Note, however, that in order to find via the gap-closing the same phase boundaries as in the above mean-field calculation it is mandatory to take these fluctuations into account.

8.5 Low-energy theories

We now have a good understanding of the phases of the Bose Hubbard model. For weak interactions we have a superfluid that is very similar to a free-space Bose Einstein condensate. For very strong interactions there is a series of insulating Mott lobes, one for each integer filling. Moreover, we know that the generic excitations are either phonons or gapped particles and holes. However, all these pictures are only valid for the two extreme cases $U \gg t$ and $U \ll t$. In this section we try to understand the region in between. To this end, we derive from the Bose Hubbard model a long-wave length effective theory.

We will derive the effective low-energy theory using general arguments and a simple trick. While the answer is solid, there are more formal ways to derive this theory. However, it is also insightful to follow the somewhat “hand wavy” argumentation here. Let us start from the weakly interaction regime. In this case we learned that the coherence length (6.22) is given by

$$\xi = \bar{a} \sqrt{\frac{t}{U\rho}} \gg \bar{a} \quad \text{for } t \ll U, \quad (8.52)$$

where \bar{a} is the lattice constant. In this case we expect typical variations to happen on much larger scale than the lattice constant. Hence, we write for our bosonic operators

$$\hat{a}_i = \hat{a}(\mathbf{x}_i) \quad \text{and} \quad \hat{a}_{i+1} \approx \hat{a}(\mathbf{x}_i) + \bar{a} \hat{a}'(\mathbf{x}_i) + \frac{\bar{a}^2}{a} \hat{a}''(\mathbf{x}_i). \quad (8.53)$$

Therefore we can write for the kinetic energy part of the Hamiltonian

$$-t\hat{a}_i^\dagger a_j \longrightarrow -t\frac{\bar{a}^2 t}{2}\hat{a}\hat{a}'' = \frac{ta^2}{2}(\hat{a}')^2. \quad (8.54)$$

In a next step we interpret the operator \hat{a} as a simple complex-valued field ψ and propose a low-energy theory of the form

$$\mathcal{L}_{\text{GPE}} = \eta i\psi^* \partial_t \psi + t\bar{a}^2 |\nabla \psi|^2 + \mu|\psi| - \frac{U}{4}|\psi|^4. \quad (8.55)$$

So far we only motivated the kinetic term. The local terms $\propto \mu, U$ are simple to understand. However, the first term $\propto \eta = \pm$ needs further explanation. In order to gain a better understanding we use the above Lagrangian to derive equations of motions for the field ψ

$$\frac{\partial}{\partial t} \frac{\partial \mathcal{L}_{\text{GPE}}}{\partial \partial_t \psi^*} + \nabla \frac{\partial \mathcal{L}_{\text{GPE}}}{\partial \nabla \psi^*} - \frac{\partial \mathcal{L}_{\text{GPE}}}{\partial \psi^*} = 0 \quad \Rightarrow \quad \eta i\dot{\psi} = -t\bar{a}^2 \psi'' - \mu\psi + \frac{U}{2}|\psi|^2 \psi, \quad (8.56)$$

where in the last line we switched to a short-hand notation $\partial_t \psi = \dot{\psi}$, $\partial_x \psi = \psi'$, etc. We recognize the long-wavelength theory as the Gross-Pitaevskii equation. This was to be expected as for weak interactions, where $\xi \gg \bar{a}$, the lattice should not play any role. However, for now, we left the phenomenological parameter η free. To fix it, we further analyze the above equation by writing

$$\psi = (\rho_0 + \delta\rho)e^{i\phi} \quad \Rightarrow \quad \dot{\psi} = \delta\dot{\rho} + i\dot{\phi}(\rho_0 + \delta\rho)e^{i\phi} \quad \text{and} \quad e^{-i\phi}\psi'' \approx \delta\rho'' + i\phi''\rho_0. \quad (8.57)$$

Inserting this into the Gross-Pitaevskii equation we obtain two equations

$$I: \quad \eta\delta\dot{\rho} = -t\bar{a}^2 \rho_0 \phi'' \quad \left[\partial_t \rho = -\nabla J \right] \quad (8.58)$$

$$\Rightarrow \eta: \quad \text{“particle” or “hole” condensate} \quad (8.59)$$

The comparison with the continuity equation helped us to identify that η encodes if we deal with a condensate of particles or holes! The second equation reads

$$II: \quad -\eta\dot{\phi}\rho_0 = -t\bar{a}^2 \delta\rho'' - \mu(\rho_0 + \delta\rho) + \frac{U}{2}(\rho_0 + \delta\rho)^3 \quad (8.60)$$

We first deal with static solutions where $\partial_t \dots = 0$.

$$-\mu\rho_0 + \frac{U}{2}\rho_0^3 = 0 \quad \Rightarrow \quad \rho_0 = \sqrt{\frac{2\mu}{U}} \quad \text{or} \quad \mu = \frac{U}{2}\rho_0^2 \quad (8.61)$$

Hence we find the old result relating U to the density.² To solve for the time-dependent solution we take the time derivative of II to get

$$-\eta\rho_0\ddot{\phi} = -t\bar{a}^2 \delta\dot{\rho}'' - \mu\delta\dot{\rho} + \frac{3U}{2}\rho_0^2 \delta\dot{\rho} \stackrel{I}{\Rightarrow} \quad (8.62)$$

$$\ddot{\phi} = t\bar{a}^2 \phi'''' + \mu t\bar{a}^2 \phi'' + \frac{3U}{2}\rho_0^2 t\bar{a}^2 \phi'' \stackrel{(8.61)}{\Rightarrow} \quad (8.63)$$

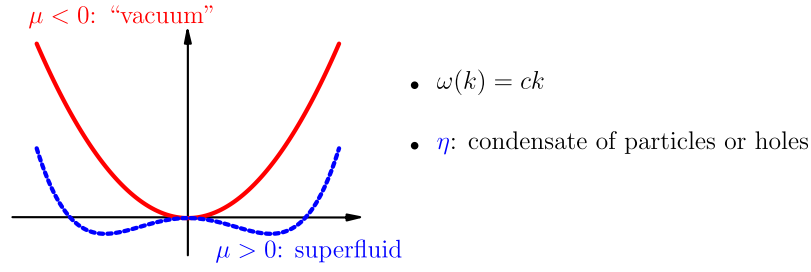
$$\ddot{\phi} \approx -Ut\bar{a}^2 \phi''. \quad (8.64)$$

And hence

$$\omega_{\text{GPE}}(k) = \sqrt{Ut\bar{a}^2}|\mathbf{k}|. \quad (8.65)$$

We recovered the phonon dispersion that we also obtained from the microscopic description of the condensate. However, here we get only the long-wavelength part as we are constrained to $k \ll 1/\xi$. We summarize our findings with the following figure:

²note that ρ_0 is the square root of the density in our notation here.



8.5.1 Relativistic low-energy theory

With the effective action \mathcal{L}_{GPE} at hand we can now address the transition region. We saw that the sign of η determines whether we deal with a particle or a hole condensate. Moreover, we know that at the lower Mott boundary holes condense while at the upper boundary particles condense, see Fig. 8.6. From the figure we directly infer that the sign of η has to change at the tip of the Mott lobe. Hence, the dynamical part $\psi^* \dot{\psi}$ drops out of our low-energy theory. The only way to fix this is by introducing higher derivatives and the lowest yields the sought after effective theory of the transition at the tip of the lobe

$$\mathcal{L}_{\text{crit}} = |\partial_t \psi|^2 + |\nabla \psi|^2 + r|\psi|^2 - \frac{U}{4}|\psi|^4. \quad (8.66)$$

As mentioned above, we could also derive this theory from microscopic consideration, which however lies beyond the scope of this course. Let us just mention a few properties of this theory: (i) it has an (emergent) relativistic symmetry (space and time enter on equal footing), (ii) the transition therefore has a dynamical critical exponent of $z = 1$. (iii) The excitation spectrum is profoundly affected by the relativistic nature of the theory. Let us try to understand the last point.

The static part is the same as for the Gross-Pitaevskii equation and we immediately find

$$\rho_0 = \sqrt{\frac{-2r}{U}} \quad (8.67)$$

Let us now investigate the dynamics for the superfluid phase

$$\rho_0 \neq 0 \quad \ddot{\phi} = \phi'' \quad \Rightarrow \quad \omega \sim |k|, \quad (8.68)$$

$$\delta \dot{\rho} = \delta \rho'' - r \delta \rho + \frac{3U}{2} \rho_0^2 \delta \rho \quad \Rightarrow \quad \omega \sim \sqrt{|r|} + \frac{k^2}{2\sqrt{|r|}}. \quad (8.69)$$

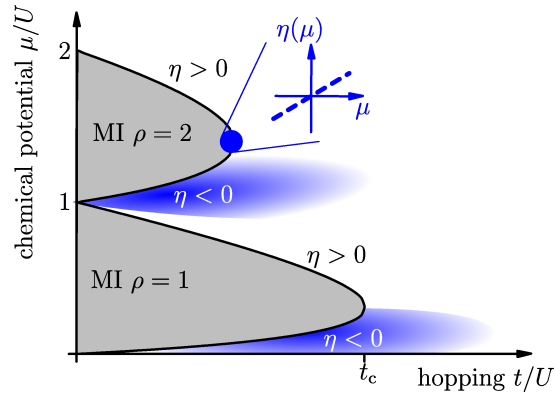


Figure 8.6: **Effective theory.**

We found, in addition to the sound mode, a massive mode that softens at the transition. It is a modulation of the amplitude ($\delta\rho$) of the order-parameter and is sometimes called the *Higgs-mode*. In the Mexican hat potential $r|\psi|^2 + |\psi|^4$ the sound mode is the modulation along the rim (Goldstone mode), while the Higgs mode is perpendicular to the rim.³ For the Mott phase we find

$$\rho_0 = 0 \quad \psi = \psi_R + i\psi_I \quad \Rightarrow \quad \ddot{\psi}_R + i\ddot{\psi}_I = \psi_R'' + i\psi_I'' + r(\psi_R + \psi_I) \quad (8.70)$$

$$\Rightarrow \omega_{R/I} = \sqrt{r} + \frac{k^2}{2\sqrt{r}}, \quad (8.71)$$

which are nothing but the particle and hole excitations.

³Ask yourself why this is not the case in the GPE limit!